ACS OMEGA

Article

Cite This: ACS Omega 2018, 3, 2715−2723

Porous Polylactide Film Plus Atorvastatin-Loaded Thermogel as an Efficient Device for Peritoneal Adhesion Prevention

Jiannan Li,[†,‡] Xiangru Feng,[†] Jian Shi,[†,‡] Tongjun Liu,[‡] and Jianxun Ding*[,†]

[†]Key Laboratory of Polymer Ecomaterials, Changchun Institute of Applied Chemistry, Chinese Academy of Sciences, 5625 Renmin Street, Changchun 130022, P. R. China

[‡]Department of General Surgery, The Second Hospital of Jilin University, 218 Ziqiang Street, Changchun 130041, P. R. China

Supporting Information

ABSTRACT: Peritoneal adhesion is a common postoperative complication that causes many kinds of organ dysfunctions. It can be minimized by the integration of physical isolation and pharmaceutical treatment. However, the gas permeability of traditional medical devices for adhesion prevention is not satisfactory, which increases the risk of infection and inflammation, thus facilitating the formation of peritoneal adhesion. In this study, a device of porous polylactide (PLA) film plus atorvastatin (ATV)-loaded thermogel was developed for peritoneal adhesion prevention. PLA film acted as a physical barrier to prevent the connection of fibrin bridges between the injured tissues and nearby normal organs. Simultaneously, ATV was released to achieve the antifibrin deposition and anti-inflammatory effect. The porous properties of PLA film and thermogel increased the gas permeability and further inhibited the inflammatory responses. The in vivo study demonstrated that the porous PLA film with ATV-loaded thermogel possessed excellent anti-inflammation ability and satisfactory antiadhesion capacity, indicating its great potential for clinical application.

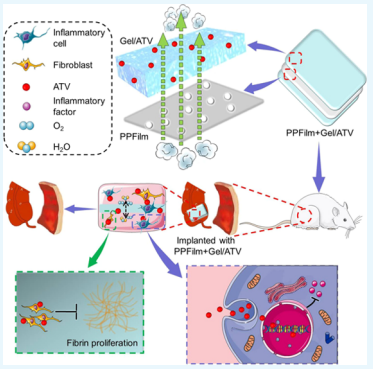

1. INTRODUCTION

Peritoneal adhesion, characterized by proliferated fibrin bands connecting the injured tissues and nearby normal organs, is a very common postoperative complication that often occurs after various peritoneal surgeries.[1,2] The adhesion bands can be classified into a diversity of types ranging from thin fibrous films to a complex of fibrous bridges, blood vessels, and nerves.[3,4] Peritoneal adhesion can lead to many physical problems in the patients, including chronic abdominal pain, bowel obstruction, infertility, and organ dysfunction.[5,6]

Even though many efforts have been made to inhibit peritoneal adhesion, such as physical isolation and pharmaceutical treatment, the exact pathophysiology is not fully understood. Many factors, involving peritoneal injuries, foreign materials, and local inflammation and infection, are thought to be associated with the formation of peritoneal adhesion.[7,8] Until now, local inflammation has been considered as the main cause of peritoneal adhesion.[9,10] Specifically, our body would probably assume that we are in a severe trauma after undergoing surgeries, which triggers the release of vasodilators, histamine, and various cytokines.[1] The permeability of blood vessels would be subsequently increased, leading to the effusion of fibrous tissues. When fibrin deposition effect is greater than fibrin degradation effect, fibrous bands will form and peritoneal adhesion will occur.[3]

With the development of tissue engineering, physical isolation based on biocompatible and biodegradable polymer materials, as well as combined utilization with antifibrin proliferation or anti-inflammation drugs, has attracted much attention in adhesion prevention.

The physical barriers, such as Seprafilm[11] and Interceed,[12] mainly prevent the adhesion formation by simply separating the injured tissues from adjacent normal organs, but have no effect on the inhibition of excessive deposition of fibrous tissues or inflammatory responses. Besides, the gas permeability of traditional physical barriers is poor, which may form a suitable environment for the proliferation of anaerobic bacteria and increase the possibility of infection and inflammatory responses. In addition, poor gas permeability will result in the deposition of excessive fibrous tissues and the formation of peritoneal adhesion, which are not beneficial for wound healing.[13]

For pharmaceutical treatment, drugs that can inhibit fibrin proliferation and inflammatory responses are often used for peritoneal adhesion prevention. For example, atorvastatin (ATV) that is usually applied for the treatment of high blood cholesterol has been reported to reduce the amounts of peritoneal fibrin bands[14,15] and inhibit the expression of inflammatory factors.[16] However, the formation of fibrous bands cannot be completely inhibited by single pharmaceutical treatment, and the residual fibrous films can still induce peritoneal adhesion.[10] So, integrating pharmaceutical treatment and physical isolation and increasing the gas permeability of the

Received: January 16, 2018
Accepted: February 22, 2018
Published: March 7, 2018

DOI: 10.1021/acsomega.8b00090
ACS Omega 2018, 3, 2715−2723

Scheme 1. Schematic Illustration of Preparation and Antiadhesion of PPFilm+Gel/ATV

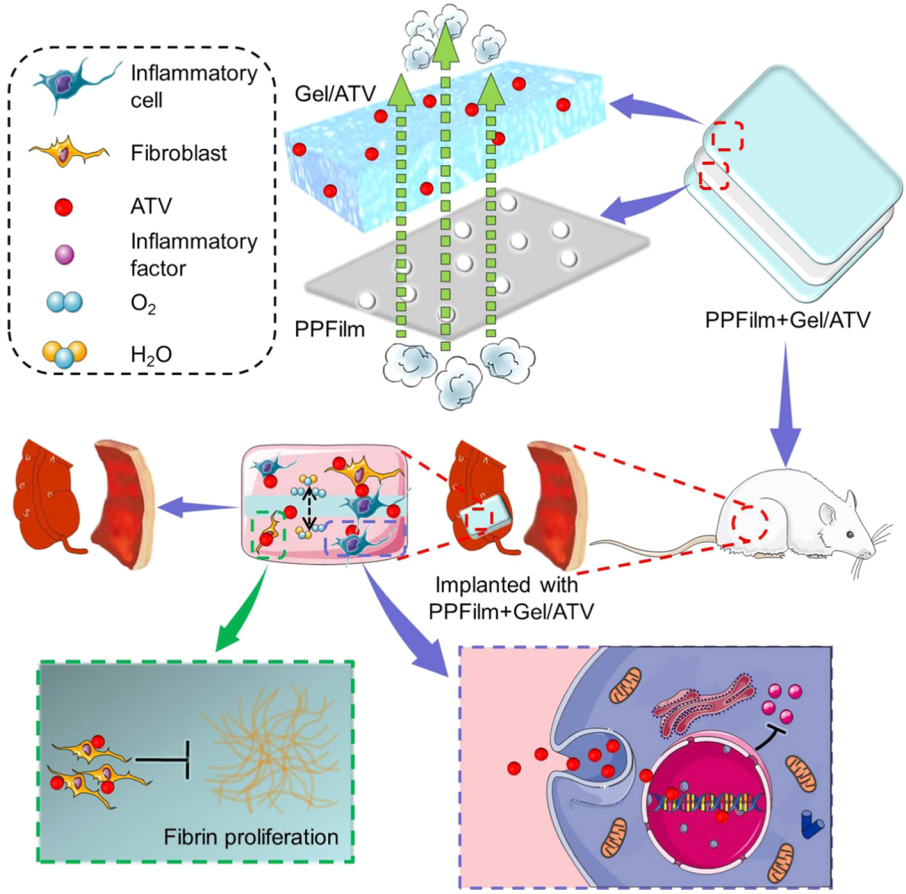

combined medical devices may provide better adhesion inhibition efficacy.

Herein, a device of porous polylactide (PLA) film with ATV-loaded thermogel was developed for the treatment of peritoneal adhesion (Scheme 1). PLA film functions as a physical barrier to separate the connection of fibrous bands between the injured areas and nearby normal tissues. In addition, the porous PLA membrane possessed high gas permeability, which might well inhibit the infection and inflammatory responses in the injured areas. For antifibrin proliferation and anti-inflammatory effect, ATV was loaded in a designed thermogel and could be continuously released. Furthermore, the thermogel also contained interconnected pores to increase gas permeability. Owing to the well-designed structure, the combination of porous PLA film and ATV-loaded thermogel might be a good solution for peritoneal adhesion prevention.

2. RESULTS

2.1. Characterizations of Membranes Plus Thermogel.

The PLA film, porous PLA film, PLA film with thermogel, PLA film with ATV-loaded thermogel, porous PLA film with thermogel, and porous PLA film with ATV-loaded thermogel were referred to as PFilm, PPFilm, PFilm+Gel, PFilm+Gel/ATV, PPFilm+Gel, and PPFilm+Gel/ATV, respectively. PFilm +Gel, PFilm+Gel/ATV, PPFilm+Gel, and PPFilm+Gel/ATV were successfully developed. Because of the temperature sensitivity, this thermogel was in liquid state at 4 °C and turned to solid at body temperature. In addition, the ATV-loaded thermogel was stable and homogeneous owing to the excellent solubility of ATV in thermogel solution at 4 °C.

The water vapor transmission rates (WVTRs) of PFilm and PPFilm were 616.86 ± 80.23 and 2101.49 ± 227.52 g m^{-2} day^{-1}, respectively. There was a significant difference between PFilm and PPFilm in WVTR, which indicated that PPFilm possessed better gas permeability in this study ($P < 0.001$).

The detailed morphologies of PFilm, PFilm+Gel, PPFilm, and PPFilm+Gel are shown in Figure 1A. PFilm showed smooth surface without obvious pores, whereas oval pores could be seen evenly distributed in PPFilm (Figure 1A). The pore size and porosity of PPFilm were about 1 μm and 75%, respectively. Furthermore, these pores were interconnected with each other. For PFilm+Gel and PPFilm+Gel, thermogel was coated on the surface of PFilm or PPFilm, and scanning electron microscopy (SEM, Inspect-F, FEI, Finland) images mainly represented the thermogel morphologies. The thermogel displayed highly porous and interconnected structure.

The stress−strain curves of PFilm, PFilm+Gel, PPFilm, and PPFilm+Gel were evaluated and are shown in Figure 1B. The curves of PFilm+Gel and PPFilm+Gel were above those of PFilm and PPFilm, which indicated that the thermogel-coated membranes possessed a stronger deformation-resistant ability than uncoated ones. In addition, the curves of PFilm and PFilm +Gel were above those of PPFilm and PPFilm+Gel. There were significant differences between PFilm and PFilm+Gel, PPFilm and PPFilm+Gel, and PFilm+Gel and PPFilm+Gel in tensile strength, Young's modulus, and elongation at break (Figure 1B).

Water contact angle tests indicated that the four separating films were all hydrophilic and the water contact angles of PFilm, PFilm+Gel, PPFilm, and PPFilm+Gel were 50.01 ±

DOI: 10.1021/acsomega.8b00090
ACS Omega 2018, 3, 2715−2723

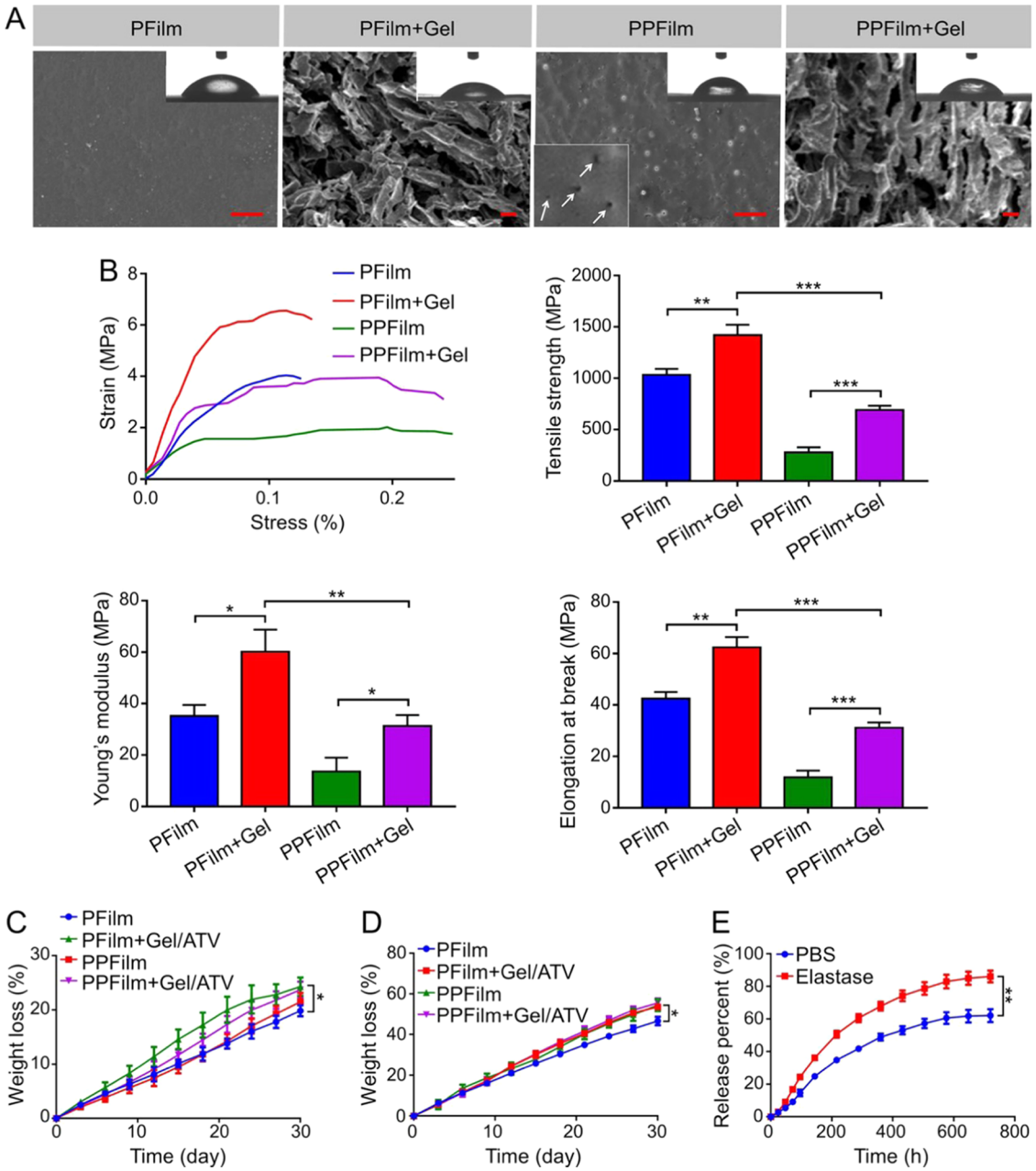

Figure 1. Morphologies, mechanical strength, degradation, and drug release behaviors of membranes and/or membranes plus thermogel. (A) SEM images and water contact angles of PFilm, PFilm+Gel, PPFilm, and PPFilm+Gel. The white arrows in the inset SEM image indicate the pores of PPFilm. (B) Mechanical properties of PFilm, PFilm+Gel, PPFilm, and PPFilm+Gel, including stress−strain curves, tensile strength, Young's modulus, and elongation at break. (C, D) Degradation behaviors of PFilm, PFilm+Gel/ATV, PPFilm, and PPFilm+Gel/ATV in PBS (C) and elastase solution (D). (E) Release of ATV from thermogel in PBS or elastase solution. Data are presented as mean ± standard deviation (SD; $n = 3$; $^{*}P < 0.05$, $^{**}P < 0.01$, $^{***}P < 0.001$). Scale bars = 10 μm.

1.62, 41.71 ± 2.82, 38.41 ± 2.42, and 37.65 ± 6.32°, respectively.

2.2. In vitro Degradation. The degradation of PFilm, PPFilm, and Gel/ATV was performed separately. Figure 1C,D shows the degradation profiles of PFilm, PPFilm, PFilm+Gel/ATV, and PPFilm+Gel/ATV in phosphate-buffered saline (PBS) or elastase solution. After degradation for 30 days, the weight losses of PFilm, PPFilm, PFilm+Gel/ATV, and PPFilm +Gel/ATV in PBS were 19.82 ± 1.03, 24.27 ± 1.69, 21.45 ± 1.66, and 23.68 ± 1.52 wt %, respectively, whereas the weight losses of PFilm, PPFilm, PFilm+Gel/ATV, and PPFilm+Gel/ATV in elastase solution were 46.62 ± 2.04, 54.53 ± 2.94, 53.64 ± 0.11, and 55.59 ± 2.22 wt %, respectively. There were no obvious differences in degradation properties among PPFilm, PFilm+Gel/ATV, and PPFilm+Gel/ATV in either PBS or elastase solution. But the degradation rate of PPFilm on day 30 was higher than that of PFilm in both incubation media ($P < 0.05$).

2.3. In vitro Drug Release. The release profiles of ATV from thermogel in PBS and elastase solution are shown in Figure 1E. Burst releases of 24.76 ± 1.35 and 36.17 ± 1.57% were detected during the first 6 days in PBS and elastase solution. Afterward, ATV was continuously and slowly released in the two incubation solutions for another 24 days. After a

DOI: 10.1021/acsomega.8b00090
ACS Omega 2018, 3, 2715−2723

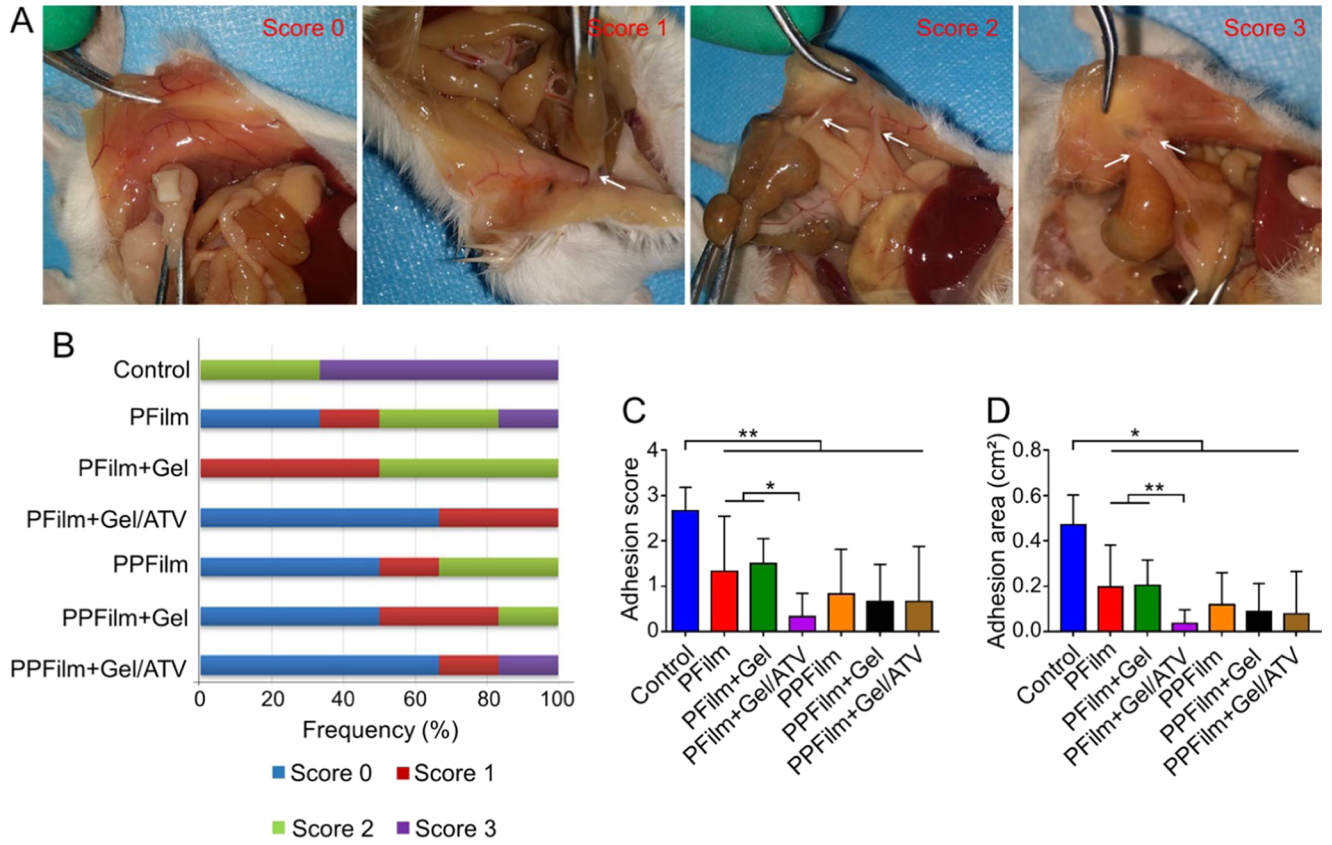

Figure 2. Antiadhesion properties of different devices. (A) Representative images of adhesion scores. The white arrows indicate the adhesion bands. (B) Distributions of adhesion scores in different groups. (C, D) Adhesion scores (C) and adhesion areas (D) in different groups. Data are presented as mean ± SD (n = 6; *P < 0.05, **P < 0.01, ***P < 0.001).

total of 30 days, about 86% of ATV was released in elastase solution, significantly higher than 62% in PBS (P < 0.01).

2.4. Animal Studies. The cecum abrasion animal model was successfully established in our study. All of the mice recovered well after surgery and none of them died before being sacrificed. All animals were kept in clean and ventilated cages with necessary human care. They were sacrificed 14 days post surgery, and the peritoneal adhesions of different groups were evaluated by gross observation and histological evaluation.

2.4.1. Gross Evaluation. The surgical wounds of mice were first examined to make sure that none of the mice was infected. Then, the abdomen was exposed and the peritoneal adhesion was observed, evaluated, and recorded. Representative adhesion scores of 0−3 were analyzed and are shown in Figure 2A. Higher adhesion scores represented more severe adhesions and increased difficulty to dissect the adhesion bands. Figure 2B shows the distributions of adhesion scores in different groups. The adhesion scores of control, PFilm, PFilm+Gel, PFilm+Gel/ATV, PPFilm, PPFilm+Gel, and PPFilm+Gel/ATV groups were 2.67 ± 0.51, 1.33 ± 1.21, 1.50 ± 0.55, 0.33 ± 0.52, 0.83 ± 0.98, 0.67 ± 0.82, and 0.67 ± 1.21, respectively. In the control group, the adhesion was extremely obvious and some adhesion bridges connected the injured areas and adjacent organs. In comparison, the adhesion scores in the other groups were lower. Specifically, PFilm+Gel/ATV induced less adhesion formation compared to PFilm+Gel and PFilm (P < 0.05). However, there were no significant differences in adhesion scores among the PPFilm, PPFilm+Gel, and PPFilm+Gel/ATV groups. Furthermore, there were also no differences between the PFilm+Gel/ATV and PPFilm+Gel/ATV groups.

The adhesion areas analyzed by Adobe Photoshop CS6 (Adobe; CA) are shown in Figure 2D. The adhesion areas of control, PFilm, PFilm+Gel, PFilm+Gel/ATV, PPFilm, PPFilm +Gel, and PPFilm+Gel/ATV groups were 0.47 ± 0.13, 0.20 ± 0.19, 0.21 ± 0.11, 0.04 ± 0.06, 0.12 ± 0.14, 0.09 ± 0.12, and 0.08 ± 0.19 cm^2, respectively. All of the other groups showed less adhesion areas compared to the control group. Mice treated with PFilm+Gel/ATV showed much alleviated adhesion compared to PFilm+Gel and PFilm (P < 0.01). The PFilm +Gel/ATV and PPFilm+Gel/ATV groups showed no statistical difference in adhesion areas. In addition, there were also no significant differences in adhesion areas among the PPFilm, PPFilm+Gel, and PPFilm+Gel/ATV groups.

2.4.2. Histological Analyses. Hematoxylin and eosin (H&E) and Masson's trichrome staining were performed to further analyze the adhesion formation and collagen deposition (Figure 3A). In the control group, there were evident adhesions between the abdomen and cecum. Besides, large amounts of polymorphonuclear cells can be observed in the control group, which represent severe inflammatory responses. On the contrary, adhesions were well prevented in mice treated with antiadhesion membranes, and only a minimal amount of collagen tissues were observed in these groups. However, the results of H&E staining were consistent with those of Masson's trichrome staining among the PFilm, PFilm+Gel, PFilm+Gel/ATV, PPFilm, PPFilm+Gel, and PPFilm+Gel/ATV groups.

2.4.3. Inflammatory Estimations. Immunofluorescence staining of inflammatory factors, e.g., tumor necrosis factor-α (TNF-α), interleukin-1 (IL-1), and interleukin-6 (IL-6), was performed to evaluate the inflammation statuses in different

DOI: 10.1021/acsomega.8b00090
ACS Omega 2018, 3, 2715−2723

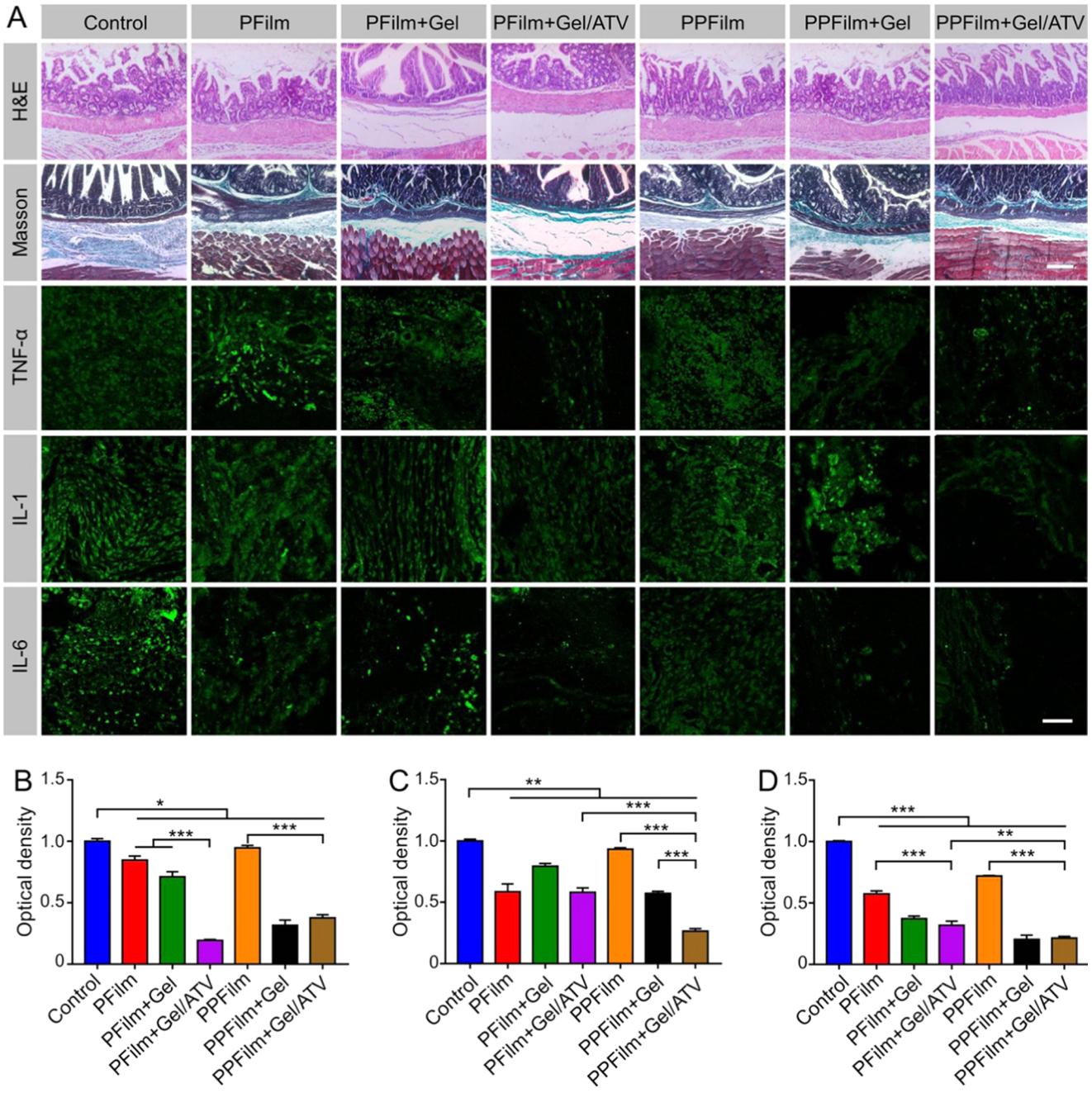

Figure 3. Histological analyses of the injured abdomen and cecum. (A) H&E and Masson's trichrome staining, and immunofluorescence profiles of TNF-α, IL-1, and IL-6 in repaired sites. (B–D) Semiquantitative analyses of TNF-α (B), IL-1 (C), and IL-6 (D). Data are presented as mean ± SD (n = 3; *P < 0.05, **P < 0.01, ***P < 0.001). Scale bars = 100 μm.

groups. Figure 3A shows the confocal laser scanning microscopy (CLSM; Carl Zeiss, LSM 780; Jena, Germany) images of each section. CLSM images revealed that the inflammatory factors were abundantly expressed in the injured cecum, abdomen, and regenerated tissues in the control group. A similar phenomenon was also found in the PFilm, PFilm +Gel, and PPFilm groups. However, in the PFilm+Gel/ATV and PPFilm+Gel/ATV groups, the expression of inflammatory factors was extremely suppressed.

To further analyze the inflammation responses, relative fluorescence intensities of TNF-α, IL-1, and IL-6 in CLSM images were calculated by ImageJ software (National Institutes of Health, Bethesda, MD) (Figure 3B–D). The fluorescence intensity of the control group was defined as "1", and the ratios of fluorescence intensities of other groups and control group were defined as the relative intensities. Compared to all of the other six groups, the control group showed higher relative fluorescence intensities of TNF-α (P < 0.05), IL-1 (P < 0.01), and IL-6 (P < 0.001). For TNF-α, the relative fluorescence intensity in the PFilm+Gel/ATV group was significantly lower than that in the PFilm and PFilm+Gel groups (P < 0.001). The relative fluorescence intensity in the PPFilm+Gel/ATV group was lower than that in the PPFilm group (P < 0.001). For IL-1, the relative fluorescence intensity was the lowest in the PPFilm +Gel/ATV group and there was statistical difference between the PFilm+Gel/ATV and PPFilm+Gel/ATV groups (P < 0.001). For IL-6, the relative fluorescence intensities in the PFilm+Gel/ATV or PPFilm+Gel/ATV group were lower than

DOI: 10.1021/acsomega.8b00090
ACS Omega 2018, 3, 2715–2723

those in the PFilm and PPFilm groups ($P < 0.001$). In addition, there was significant difference in relative fluorescence intensities between the PPFilm+Gel/ATV and PFilm+Gel/ATV groups ($P < 0.01$).

3. DISCUSSION

Postoperative abdominal adhesion is a common complication, which is very hard to prevent and can cause many kinds of organ dysfunctions. Once adhesions form, the intestines or other intra-abdominal organs may be affected, leading to functional disorders or even secondary operation. As abdominal adhesion has attracted extensive attention, traditional therapeutic strategies and tissue engineering technologies, such as early exercise, physical barriers, and pharmaceutical agents, have been well studied and applied to reduce or eliminate the peritoneal adhesion.

As physical barriers, electrospinning membranes[17,18] and hydrogels[2,19] have been extensively used in adhesion prevention to isolate the traumatized tissues from the surrounding normal organs. Furthermore, the drug-loaded physical barriers have been further explored in recent years, and the antiadhesion pharmaceutical agents, such as 5-fluorouracil,[20] celecoxib,[5,21] mitomycin-C,[22] and ATV,[14,15] have been often loaded into barriers to reinforce the antiadhesion efficiency. Among numerous drugs applied in adhesion prevention, ATV has been reported to possess both anti-inflammation and antifibrin deposition properties. Although the combination of physical barriers and pharmaceutical agents has shown excellent efficacy in adhesion prevention, the permeability of most of traditional antiadhesion devices was less satisfactory that would probably increase the possibility of infection and inflammatory responses and affect the wound healing. Medical devices with better gas permeability can keep the moisture in healing environment, exchange oxygen and water vapor well, and decrease the chances of wound infection.[23,24] As a result, applying drug-loaded physical barriers with good gas permeability may achieve better adhesion prevention capability.

In our study, we developed a device of porous PLA film with the ATV-loaded thermogel for peritoneal adhesion prevention. Herein, PLA membrane mainly separated the connection of adhesion bands between the injured sites and nearby tissues. ATV was released from the thermogel to play anti-inflammation and antifibrin deposition effects. Besides, the thermogel could absorb wound exudates because of its superior swelling ratio, and also provide a relatively wet environment.[25,26] The porous property of PLA film and thermogel increased the gas permeability, thus inhibiting the possibility of infection and inflammation, and facilitating wound healing.

WVTR was applied to detect the gas permeability of PFilm and PPFilm in this study. An ideal wound dressing would not only increase the gas circulation but also control the evaporative water loss from the wound.[27] A lower WVTR can increase the possibility of inflammatory responses, and a higher WVTR can induce the fast drying of the wound.[27] The WVTRs of PFilm and PPFilm were all within the range of 264−4800 g m^{-2} day^{-1}, which are optimal for injured tissues.[27] However, the WVTR of PPFilm (2101.49 ± 227.52 g m^{-2} day^{-1}) was significantly higher than that of PFilm (616.86 ± 80.23 g m^{-2} day^{-1}), which indicated that PPFilm possessed better gas permeability.

The surface morphologies of PPFilms tested by SEM showed evenly distributed pores. No obvious differences were found in the surface morphologies between PFilm+Gel and PPFilm +Gel, as thermogel was coated on the surface of PFilm and PPFilm. ATV was well dissolved in the thermogel solution in our study and no obvious drug crystals were detected. The fine dissolution can benefit the sustained release of ATV, a very important element for adhesion prevention. The inhomogeneous dissolvent of agents always leads to the burst release of drugs. However, the inhibition of peritoneal adhesion is a long process, so sustained and long-term drug release is necessary. Therefore, full dissolution of ATV was essential for further peritoneal adhesion prevention.

The stress−strain curves, tensile strength, Young's modulus, and elongation at break were all measured to evaluate the mechanical properties of different samples. When coated on the surface of membranes, thermogel increased the deformation-resistant ability of the membranes. However, the pores in the membrane decreased the deformation-resistant ability of the membranes. In addition, thermogel increased the tensile strength, Young's modulus, and elongation at break of the membranes, whereas the pores in the membrane had a negative effect on these factors.

When used for peritoneal adhesion prevention, any movement of the membranes may interfere in the separation effects of the fibrin bands and result in adhesion formation. Better bioadhesion ability of the barriers can help them stick to the injured area and avoid further movement during the adhesion prevention process. Water contact angle tests showed that all of the membranes were hydrophilic in this study. Better hydrophilicity can contribute to enhanced bioadhesion ability of the antiadhesion barriers and also avoid the use of sutures, which may induce unnecessary inflammation and fibrin deposition. In our previous study, we confirmed that membranes with stronger bioadhesion ability could better inhibit inflammation responses and possessed satisfactory adhesion prevention property.[10] The excellent hydrophilicity of the samples in this study demonstrated their satisfactory bioadhesion ability that might benefit the antiadhesion effects.

Biodegradability is another important factor for the antiadhesion application of physical barriers.[7] In our study, biodegradability of different membranes was analyzed by incubation in PBS or elastase solution for a certain period of time, and their weight losses were calculated and recorded. The general biodegradation rates exhibited a steep increase in elastase solution compared to that in PBS. This is attributed to the property of elastase solution that is inclined to degrade polymer matrices rapidly. After incubation for 30 days, the weight losses of the samples in PBS (about 20%) were much lower than those in elastase solution (more than 50%). Interestingly, coating of thermogel on the membrane surfaces did not obviously change their biodegradation process. The thermogel-coated membranes showed similar biodegradation properties to non-thermogel-coated ones in both incubation media. This might be explained by the similar degradation profiles of PLA membranes to the thermogel in this study. PPFilm degraded more quickly than PFilm in PBS and elastase solution. This might result from the structural characterizations of PPFilm that the evenly distributed pores increased the contact area between PPFilm and the incubation media, thus accelerating the degradation process. Many factors (e.g., polymers, pore sizes, porosity, thickness of membranes) can influence the degradation rate of polymer barriers.[28,29] Unlike other PLA-based electrospun membranes, we did not observe obvious pores composed of interwined fibers, even when the PLA membrane was magnified 1000 times. This basic structure

DOI: 10.1021/acsomega.8b00090
ACS Omega 2018, 3, 2715−2723

of PLA film may decrease the degradation rate in our study. However, there was still about 50% weight loss of PLA film after degradation for 30 days in elastase solution. We hypothesize that the complete degradation time of the PLA membrane might be less than 60 days because the degraded PLA film can be infiltrated with incubation medium and the degradation process can be accelerated.[28]

Sustained drug release from the thermogel is an essential requirement for efficient adhesion prevention. Therefore, the drug release behavior of ATV was also analyzed in PBS and elastase solution. As expected, elastase accelerated the drug release, which was consistent with the degradation properties, and demonstrated the correlation between degradation and release profiles. Similar to the release behaviors of agents incorporated in adhesion prevention barriers in other studies, the release of ATV was characterized by either of the two patterns, the burst release or sustained release.[30,31] In elastase solution, the burst release of ATV was not obvious and only about 35% amount of ATV was released for the first 6 days. This was because of the good dissolution of ATV in the thermogel. Sustained release of ATV was followed for the next few days, and more than 60% of ATV was released 14 days post surgery. In the peritoneal adhesion prevention process, long-term drug treatment is necessary to inhibit the inflammatory responses and predictively contribute to prevent peritoneal adhesion.[1]

The antiadhesion capabilities of various membranes in vivo were evaluated in a cecum-abdominal animal model. Compared to the control group, the adhesion scores and adhesion areas were lower in all experimental groups. This was because peritoneal adhesions were inhibited by physical isolation and/or pharmaceutical treatment. Because of the combination of physical barrier effect of the membrane, and anti-inflammation and antifibrin deposition effects of ATV, the adhesion scores and areas decreased more obviously in the PFilm+Gel/ATV group than those in the PFilm and PFilm+Gel groups. However, there were no statistical differences in adhesion formation among the PFilm+Gel/ATV, PPFilm, PPFilm+Gel, and PPFilm+Gel/ATV groups. All of the PPFilm, PPFilm+Gel, and PPFilm+Gel/ATV groups showed excellent antiadhesion efficacy. This might be explained by that the porous PLA film exhibited excellent adhesion prevention effect, in which the membrane acted as the physical isolation and the oval pores increased the gas permeability and provided a suitable environment for wound healing.[32] Through increasing the gas circulation in the injured area, the accumulation of exudates can be decreased, the proliferation of anaerobic bacteria can be inhibited, and the inflammation responses can be well prevented.[32] As a result, PPFilm dramatically decreased the peritoneal adhesion, whereas the use of ATV-loaded thermogel did not increase the adhesion prevention ability of PPFilm in our study.

Consistent with the results of gross pathology, H&E and Masson's trichrome staining experiments did not reveal any superiority of PPFilm+Gel/ATV in adhesion prevention compared to PPFilm. We further evaluate the inflammation inhibition effects of the samples used in our study as an important factor for antiadhesion applications. TNF-α, IL-1, and IL-6 are the three most important proinflammatory cytokines participating in the immune process. TNF-α can trigger the release of IL-1 and IL-6. These three factors can increase the permeability of blood vessels, and the production of oxygen radicals and other proinflammatory factors.[33] The secretions of these three factors were evaluated by CLSM and semiquantitative analyses (Figure 3). For IL-1 and IL-6, the relative fluorescence intensity of PPFilm+Gel/ATV was lower than that of PFilm+Gel/ATV. This might attribute to the fact that the pores increased the gas permeability, decreased the accumulation of exudates, and further inhibited the inflammatory responses. The best anti-inflammatory effect was observed in the PPFilm+Gel/ATV group. The expressions of these three factors were obviously suppressed compared to other groups. However, decreased inflammatory responses did not lead to increased adhesion prevention effect. Just as discussed above, PPFilm exhibited high antiadhesion ability, and the decreased inflammatory responses did not increase the peritoneal adhesion prevention efficacy.

4. CONCLUSIONS

In this study, an antiadhesion device composed of porous PLA film with ATV-loaded thermogel was successfully prepared. This medical device integrated the physical isolation and pharmaceutical treatment and possessed high gas permeability property for effective antiadhesion. PLA film inhibited the connection of adhesion bands between injured areas and adjacent normal organs. ATV was released sustainably to play antifibrin deposition and anti-inflammatory effects. The porous property of PPFilm+Gel/ATV further inhibited the inflammatory responses and prevented the formation of peritoneal adhesion. PPFilm+Gel/ATV showed high anti-inflammation ability and antiadhesion effect. All of the results demonstrated the superiority of PPFilm+Gel/ATV in the application of peritoneal adhesion prevention.

5. MATERIALS AND METHODS

5.1. Materials. PFilm, PPFilm, and the methoxy poly(ethylene glycol)-*block*-poly(lactide-*co*-glycolide) thermogel were provided by Changchun SinoBiomaterials Co., Ltd. (Changchun, P. R. China). ATV and elastase were purchased from Aladdin Reagent Co., Ltd. (Shanghai, P. R. China). Tween-80 was bought from Sigma-Aldrich (Shanghai, P. R. China). The primary antibodies of TNF-α, IL-1, and IL-6 were purchased from Abcam (Cambridge, MA).

5.2. Preparations of Porous PLA Film Plus ATV-Loaded Thermogel. The thermogel was in a sol state at 4 °C while changed to a gel state at body temperature. Thermogel solution (20.0 wt %) was acquired by dissolving the thermogel in PBS at 4 °C. ATV (10.0 wt %) with respect to the amount of thermogel was added to the above solution and stirred well at 4 °C for about 24 h. ATV-loaded thermogel (100.0 μL) was applied evenly on the surface of 1.0 × 1.0 cm^2 sized porous membrane to obtain PPFilm+Gel/ATV as an advanced device. For comparison, PFilm+Gel, PFilm+Gel/ATV, and PPFilm+Gel were also developed.

5.3. Water Vapor Transmission Rate. The WVTRs of PFilm and PPFilm were measured according to a previous study.[34] In detail, PFilm or PPFilm was put as a cap on the mouth of a cup of 26 mm diameter. The cup containing 10.0 mL of distilled water was then incubated in a constant temperature and humidity chamber (37 °C and 50% RH). WVTR was calculated as WVTR = $(\Delta m)/(At)$, where Δm, A, and t are the weight change of each cup, contact area, and incubation time, respectively.

DOI: 10.1021/acsomega.8b00090
ACS Omega 2018, 3, 2715−2723

■ ASSOCIATED CONTENT

Supporting Information

The Supporting Information is available free of charge on the ACS Publications website at DOI: 10.1021/acsomega.8b00090.

Experimental protocols about characterizations of membranes plus thermogel, in vitro degradation, drug release study, and animal studies (PDF)

■ AUTHOR INFORMATION

Corresponding Author

*E-mail: jxding@ciac.ac.cn.

ORCID

Jianxun Ding: 0000-0002-5232-8863

Notes

The authors declare no competing financial interest.

■ ACKNOWLEDGMENTS

This research was financially supported by the National Natural Science Foundation of China (Grant Nos. 51673190, 51603204, 51673187, 21474012, 51273037, and 51520105004) and the Science and Technology Development Program of Jilin Province (Grant Nos. 20160204015SF and 20160204018SF). All authors sincerely thank Prof. Xuesi Chen from Changchun Institute of Applied Chemistry, Chinese Academy of Sciences, for his kind help with the manuscript revision.

■ REFERENCES

(1) Li, J.; Feng, X.; Liu, B.; Yu, Y.; Sun, L.; Liu, T.; Wang, Y.; Ding, J.; Chen, X. Polymer materials for prevention of postoperative adhesion. *Acta Biomater.* **2017**, *61*, 21−40.

(2) Yang, Y.; Liu, X.; Li, Y.; Wang, Y.; Bao, C.; Chen, Y.; Lin, Q.; Zhu, L. A postoperative anti-adhesion barrier based on photoinduced imine-crosslinking hydrogel with tissue-adhesive ability. *Acta Biomater.* **2017**, *62*, 199−209.

(3) Arung, W.; Meurisse, M.; Detry, O. Pathophysiology and prevention of postoperative peritoneal adhesions. *World J. Gastroenterol.* **2011**, *17*, 4545−4553.

(4) Moris, D.; Chakedis, J.; Rahnemai-Azar, A. A.; Wilson, A.; Hennessy, M. M.; Athanasiou, A.; Beal, E. W.; Argyrou, C.; Felekouras, E.; Pawlik, T. M. Postoperative abdominal adhesions: Clinical significance and advances in prevention and management. *J. Gastrointest. Surg.* **2017**, *21*, 1713−1722.

(5) Jiang, S.; Zhao, X.; Chen, S.; Pan, G.; Song, J.; He, N.; Li, F.; Cui, W.; Fan, C. Down-regulating ERK1/2 and SMAD2/3 phosphorylation by physical barrier of celecoxib-loaded electrospun fibrous membranes prevents tendon adhesions. *Biomaterials* **2014**, *35*, 9920−9929.

(6) De Clercq, K.; Schelfhout, C.; Bracke, M.; De Wever, O.; Van Bockstal, M.; Ceelen, W.; Remon, J. P.; Vervaet, C. Genipin-crosslinked gelatin microspheres as a strategy to prevent postsurgical peritoneal adhesions: *In vitro* and in vivo characterization. *Biomaterials* **2016**, *96*, 33−46.

(7) Wu, W.; Cheng, R.; das Neves, J.; Tanga, J.; Xiao, J.; Ni, Q.; Liu, X.; Pan, G.; Li, D.; Cui, W.; Sarmento, B. Advances in biomaterials for preventing tissue adhesion. *J. Controlled Release* **2017**, *261*, 318−336.

(8) Hu, W.; Lu, S.; Ma, Y.; Ren, P.; Ma, X.; Zhou, N.; Zhang, T.; Ji, Z. Poly(dopamine)-inspired surface functionalization of polypropylene tissue mesh for prevention of intra-peritoneal adhesion formation. *J. Mater. Chem. B* **2017**, *5*, 575−585.

(9) Shi, B.; Ding, J.; Wei, J.; Fu, C.; Zhuang, X.; Chen, X. Drug-incorporated electrospun fibers efficiently prevent postoperative adhesion. *Curr. Pharm. Des.* **2015**, *21*, 1960−1966.

(10) Li, J.; Xu, W.; Chen, J.; Li, D.; Zhang, K.; Liu, T.; Ding, J.; Chen, X. Highly bioadhesive polymer membrane continuously releases cytostatic and anti-inflammatory drugs for peritoneal adhesion prevention. *ACS Biomater. Sci. Eng.* **2017**, DOI: 10.1021/acsbiomaterials.7b00605.

(11) Nohuz, E.; Alaboud, M.; Darcha, C.; Alloui, A.; Aublet-Cuvelier, B.; Jacquetin, B. Effectiveness of hyalobarrier and seprafilm to prevent polypropylene mesh shrinkage: A macroscopic and histological experimental study. *Int. Urogynecol. J.* **2014**, *25*, 1081−1087.

(12) Poehnert, D.; Grethe, L.; Maegel, L.; Jonigk, D.; Lippmann, T.; Kaltenborn, A.; Schrem, H.; Klempnauer, J.; Winny, M. Evaluation of the effectiveness of peritoneal adhesion prevention devices in a rat model. *Int. J. Med. Sci.* **2016**, *13*, 524−532.

(13) Roy, N.; Saha, N.; Humpolicek, P.; Saha, P. Permeability and biocompatibility of novel medicated hydrogel wound dressings. *Soft Mater.* **2010**, *8*, 338−357.

(14) Dinarvand, P.; Farhadian, S.; Seyedjafari, E.; Shafiee, A.; Jalali, A.; Sanaei-rad, P.; Dinarvand, B.; Soleimani, M. Novel approach to reduce postsurgical adhesions to a minimum: Administration of losartan plus atorvastatin intraperitoneally. *J. Surg. Res.* **2013**, *181*, 91−98.

(15) Lalountas, M. A.; Ballas, K. D.; Skouras, C.; Asteriou, C.; Kontoulis, T.; Pissas, D.; Triantafyllou, A.; Sakantamis, A. K. Preventing intraperitoneal adhesions with atorvastatin and sodium hyaluronate/carboxymethylcellulose: A comparative study in rats. *Am. J. Surg.* **2010**, *200*, 118−123.

(16) Ye, H.; He, F.; Fei, X.; Lou, Y.; Wang, S.; Yang, R.; Hu, Y.; Chen, X. High-dose atorvastatin reloading before percutaneous coronary intervention increased circulating endothelial progenitor cells and reduced inflammatory cytokine expression during the perioperative period. *J. Cardiovasc. Pharmacol. Ther.* **2014**, *19*, 290−295.

(17) Chen, C. H.; Chen, S. H.; Shalumon, K. T.; Chen, J. P. Dual functional core-sheath electrospun hyaluronic acid/polycaprolactone nanofibrous membranes embedded with silver nanoparticles for prevention of peritendinous adhesion. *Acta Biomater.* **2015**, *26*, 225−235.

(18) Sheu, C.; Shalumon, K. T.; Chen, C. H.; Kuo, C. Y.; Fong, Y. T.; Chen, J. P. Dual crosslinked hyaluronic acid nanofibrous membranes for prolonged prevention of post-surgical peritoneal adhesion. *J. Mater. Chem. B* **2016**, *4*, 6680−6693.

(19) Cheng, H.; Yue, K.; Kazemzadeh-Narbat, M.; Liu, Y.; Khalilpour, A.; Li, B.; Zhang, Y. S.; Annabi, N.; Khademhosseini, A. Mussel-inspired multifunctional hydrogel coating for prevention of infections and enhanced osteogenesis. *ACS Appl. Mater. Interfaces* **2017**, *9*, 11428−11439.

(20) Yuan, B.; He, C.; Dong, X.; Wang, J.; Gao, Z.; Wang, Q.; Tian, H.; Chen, X. 5-Fluorouracil loaded thermosensitive PLGA−PEG−PLGA hydrogels for the prevention of postoperative tendon adhesion. *RSC Adv.* **2015**, *5*, 25295−25303.

(21) Li, L.; Zheng, X.; Fan, D.; Yu, S.; Wu, D.; Fan, C.; Cui, W.; Ruan, H. Release of celecoxib from a bi-layer biomimetic tendon sheath to prevent tissue adhesion. *Mater. Sci. Eng., C* **2016**, *61*, 220−226.

(22) Zhao, X.; Jiang, S.; Liu, S.; Chen, S.; Lin, Z. Y.; Pan, G.; He, F.; Li, F.; Fan, C.; Cui, W. Optimization of intrinsic and extrinsic tendon healing through controllable water-soluble mitomycin-C release from electrospun fibers by mediating adhesion-related gene expression. *Biomaterials* **2015**, *61*, 61−74.

(23) Rakhshaei, R.; Namazi, H. A potential bioactive wound dressing based on carboxymethyl cellulose/ZnO impregnated MCM-41 nanocomposite hydrogel. *Mater. Sci. Eng., C* **2017**, *73*, 456−464.

(24) Napavichayanun, S.; Amornsudthiwat, P.; Pienpinijtham, P.; Aramwit, P. Interaction and effectiveness of antimicrobials along with healing-promoting agents in a novel biocellulose wound dressing. *Mater. Sci. Eng., C* **2015**, *55*, 95−104.

(25) Bhowmick, S.; Koul, V. Assessment of PVA/silver nanocomposite hydrogel patch as antimicrobial dressing scaffold: Synthesis, characterization and biological evaluation. *Mater. Sci. Eng., C* **2016**, *59*, 109−119.

(26) Mogoşanu, G. D.; Grumezescu, A. M. Natural and synthetic polymers for wounds and burns dressing. *Int. J. Pharm.* **2014**, *463*, 127−136.
(27) Gonzalez, J. S.; Luduena, L. N.; Ponce, A.; Alvarez, V. A. Poly(vinyl alcohol)/cellulose nanowhiskers nanocomposite hydrogels for potential wound dressings. *Mater. Sci. Eng., C* **2014**, *34*, 54−61.
(28) Song, Z.; Shi, B.; Ding, J.; Zhuang, X.; Zhang, X.; Fu, C.; Chen, X. A comparative study of preventing postoperative tendon adhesion using electrospun polyester membranes with different degradation kinetics. *Sci. China: Chem.* **2015**, *58*, 1159−1168.
(29) Saha, S. K.; Tsuji, H. Hydrolytic degradation of amorphous films of L-lactide copolymers with glycolide and D-lactide. *Macromol. Mater. Eng.* **2006**, *291*, 357−368.
(30) Liu, S.; Hu, C.; Li, F.; Li, X. J.; Cui, W.; Fan, C. Prevention of peritendinous adhesions with electrospun ibuprofen-loaded poly(L-lactic acid)-polyethylene glycol fibrous membranes. *Tissue Eng., Part A* **2013**, *19*, 529−537.
(31) Chen, S.; Wang, G.; Wu, T.; Zhao, X.; Liu, S.; Li, G.; Cui, W.; Fan, C. Silver nanoparticles/ibuprofen-loaded poly(L-lactide) fibrous membrane: Anti-infection and anti-adhesion effects. *Int. J. Mol. Sci.* **2014**, *15*, 14014−14025.
(32) Song, X.; Mei, J.; Zhang, X.; Wang, L.; Singh, G.; Xing, M. M. Q.; Qiu, X. Flexible and highly interconnected, multi-scale patterned chitosan porous membrane produced in situ from mussel shell to accelerate wound healing. *Biomater. Sci.* **2017**, *5*, 1101−1111.
(33) Chung, M. Y.; Jung, S. K.; Lee, H. J.; Shon, D. H.; Kim, H. K. Ethanol extract of sarcodon asparatus mitigates inflammatory responses in lipopolysaccharide-challenged mice and murine macrophages. *J. Med. Food* **2015**, *18*, 1198−1206.
(34) Díez-Pascual, A. M.; Diez-Vicente, A. L. Wound healing bionanocomposites based on castor oil polymeric films reinforced with chitosan-modified ZnO nanoparticles. *Biomacromolecules* **2015**, *16*, 2631−2644.

DOI: 10.1021/acsomega.8b00090
ACS Omega 2018, 3, 2715−2723